

Development of an Open Architecture Capacitive Discharge Welding System

Jerry E. Gould and Sam Lewis

EWI

Abstract

Capacitive discharge (CD) welding is a variation of resistance projection welding (RPW). For CD welding, electrical power is stored in a capacitor, and discharged through a transformer into the workpieces. Of particular concern are the types of transformers used with CD welding. These typically only have very limited turns-ratios for mating the capacitor-based power with the workpieces. In this work, an open architecture CD welding system has been designed, assembled, and demonstrated. The system is specifically designed to integrate with a stacked-core transformer arrangement embedded in an existing welding frame. This arrangement allows 128 separate tap settings with windings ratios from 75:1 up to 1625:1. The system has been used to examine the CD weldability of a representative weld nut. Current range trials were conducted with two separate turns-ratios, implying separate rise times. Resulting joints were primarily evaluated for push-off strength. Samples made at best conditions were also examined metallographically. Results of these two separate trials showed similar current range behavior. However, those made with the longer rise times showed significantly higher (30%) strengths. Those welds also showed significantly greater set-downs and heat penetration into the components. Analysis of the mechanical elements of the welding system suggested that this performance variation was associated with a mismatch between how the force was applied and speed of current application. The analysis further demonstrated how such an open architecture system can be used to match characteristics of the primary power supply, transformer, and secondary configuration to achieve best practices for a selected application.

Introduction

Capacitive Discharge (CD) welding is nominally a variant of the resistance projection welding (RPW) process. These processes all incorporate a geometric feature on one or both the components to be joined allowing localization of current flow for heating and subsequent bonding⁽¹⁾. All processes in this class deliver relatively high current densities into the workpiece accomplishing heating to forging temperatures over a timeframe of 1s to 100s of milliseconds. Most systems in this class achieve the desired currents through the use of welding transformers. Such variants include alternating current (AC), primary rectified direct current, secondary rectified direct current, and more recently, medium frequency direct current. Such systems draw power for welding directly from a plant electrical system. Welding is then controlled by the magnitude and duration of that current.

CD welding is different in that this current is delivered notionally from energy stored in designed capacitor banks. During welding, the capacitors are discharged through a transformer into the workpiece⁽²⁻⁵⁾. A schematic output waveform for this process is shown in Figure 1. This

waveform typically shows a very rapid rise time (t_p) to a peak current (I_p) with a much more gradual decrease after this level has been achieved. As suggested above, CD welding is predominantly done as a variant of RPW. The result is a solid-state joining^(2,3,5), characterized by forging of the projection into the opposing substrate.

Capacitive discharge welding is used in an array of applications including specialized automotive components, industrial instruments, etc.; however, broader application of the technology has been limited by a number of factors. These include aspects such as scale of the equipment (physical size of the power supplies), cost, and system flexibility.

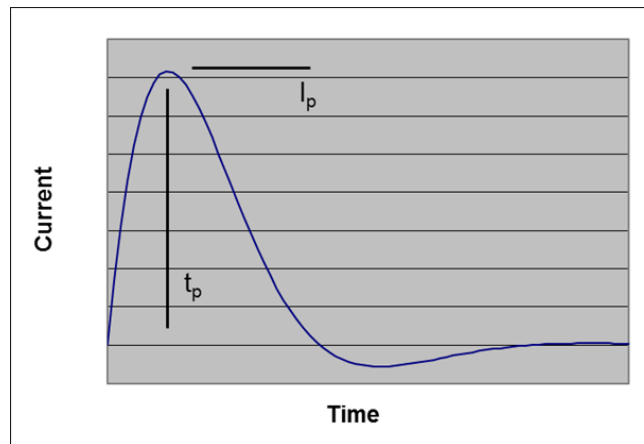


Figure 1. Schematic Secondary Current Waveform for CD Welding (chief characteristics of the waveform are the peak current (I_p) and rise time to that value (t_p))

This latter point is the central focus of this research. Most production CD welding systems in use today employ air core style transformers for matching capacitor output to the workpiece load⁽³⁾. This is necessary as the delivered power is notionally uni-polar, preventing the use of more flexible stacked core transformers. Of note, previous efforts to use stacked core transformers for CD welding required air-gaps in the core⁽⁶⁾ or use of reverse polarity pre-pulses⁽⁷⁾ to prevent saturation. The result, however, is that there is often insufficient matching between capabilities of the power supply and the requirements of the application. This work addresses development of a research CD welding system mating an open access, capacitor-based power supply to a multi-tap stacked core transformer arrangement. The configuration permits investigations into variations of capacitor arrangements and transformer windings ratios, as well as changes to both electrical and mechanical aspects of the welder secondary. The specific research described here includes development of the electrical aspects of the system, as well as preliminary assessments of achievable process variations on a selected application.

Analysis of Capacitor Discharge Welding Electrical Response

A schematic representation of the electrical circuit for capacitor discharge welding is provided in Figure 2. The circuit includes a primary capacitor (C), charged to an initial voltage (V_o), a transformer with windings ratio (N), a secondary inductance (L_s), and a load resistance (R_s). V_o (volts), C (farads), N (L_s (henrys)), and R_s (ohms) are the charge voltage, capacitance,

transformer turns-ratio, secondary inductance, and load resistance, respectively. Appropriate units are included in parenthesis for each term.

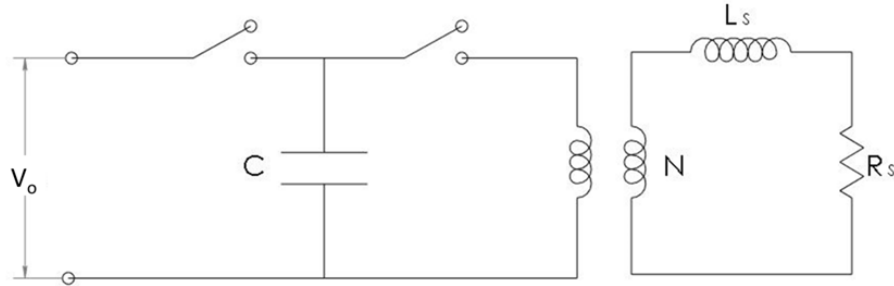


Figure 2. Schematic Representation of a Capacitive Discharge Welding Circuit

The current response of this circuit can be analyzed by reflecting the primary elements (capacitance, charge voltage) onto the secondary. The basic approach has been employed previously using phaser analysis to estimate magnetic fluxes in welding transformers⁽⁶⁾. The governing differential equation then becomes:

$$L_s \frac{d^2q}{dt^2} + R_s \frac{dq}{dt} + \frac{1}{N^2C} q = 0 \quad (1)$$

Where q (*coulombs*) is the charge value. Since this is a homogeneous differential equation, both sides can be differentiated with respect to time, yielding:

$$L_s \frac{d^2I}{dt^2} + R_s \frac{dI}{dt} + \frac{1}{N^2C} I = 0 \quad (2)$$

In this equation, I (*amps*) is the secondary current. Depending on the specific values of the circuit elements, the response may be under-, critically-, or over-damped. The under- and over-damped responses are provided in Table 1 below.

Table 1. Welding Electrical Response Solutions

Under-Damped Solution	Over-Damped Solution
$I_s(t) = V \sqrt{\frac{C}{L_s}} e^{-\zeta\omega t} \sin(\omega t) \quad \text{Eqn. 3}$	$I_s(t) = \left(\frac{V}{2NL_s} \right) \frac{e^{s_1 t} - e^{s_2 t}}{\left(\left(\frac{R_s}{2L_s} \right)^2 - \omega^2 \right)^{1/2}} \quad \text{Eqn. 5}$
$\zeta = \frac{NR_s}{2} \sqrt{\frac{C}{L_s}} \quad \text{Eqn. 4}$	$s_1 = -\frac{R_s}{2L_s} + \sqrt{\frac{R_s^2}{4L_s^2} - \frac{1}{N^2L_sC}} \quad \text{Eqn. 6}$
	$s_2 = -\frac{R_s}{2L_s} - \sqrt{\frac{R_s^2}{4L_s^2} - \frac{1}{N^2L_sC}} \quad \text{Eqn. 7}$

For both solutions, ω (Hz) is the natural frequency of the system and defined as:

$$\omega = \sqrt{\frac{1}{N^2 L_s C}} \quad (8)$$

These equations can be used to assess the influence of key system factors on the resulting secondary current waveforms. Examples are shown in Figures 3 and 4. Figure 3 represents a candidate CD power supply arrangement operating nominally at 1500 V charge voltage, a 200:1 transformer turns-ratio, a workpiece resistance of 80 $\mu\Omega$, and a secondary inductance of 760 pH as the capacitance is increased from 1000 up to 3000 μF . Of note is that the peak current increases by roughly 50%, but the rise time nearly doubles. The effect of transformer turns-ratio is shown in Figure 4. This plot is based on similar settings, but with the capacitance fixed at 2000 μF and turns-ratio decreasing from 139:1 down to 75:1. Here it can be seen that small changes in windings ratio can significantly affect the resultant rise time with minimal effect on the peak delivered currents. This ability of the turns-ratio to influence rise time relatively independent of peak current creates a control feature that can mitigate other system variables. This assessment is a key motivating factor for the work described here.

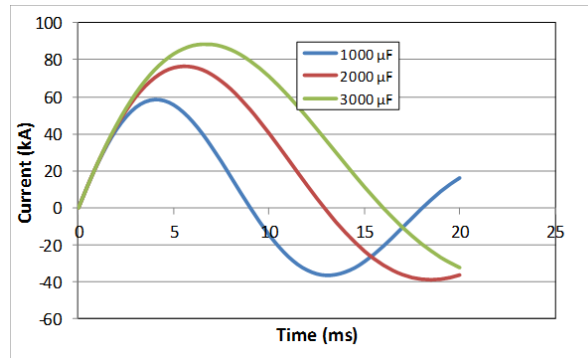


Figure 3. Influence of System Capacitance on Current Flow for CD welding ($V_c = 1500\text{V}$, $N = 200:1$, $R_s = 80 \mu\Omega$, $L_s = 760 \text{pH}$)

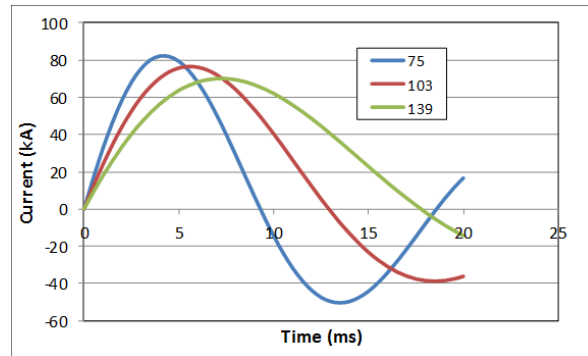


Figure 4. Influence of Windings Ratio on Current Flow for CD Welding ($V_c = 1500\text{V}$, $C = 2000 \mu\text{F}$, $R_s = 80 \mu\Omega$, $L_s = 760 \text{pH}$)

Design of the Open Architecture CD Circuitry

The baseline power supply was primarily intended to allow maximum internal flexibility (variations in capacitors, charge voltages) while interfacing with existing welding equipment incorporating stacked core transformers. The resulting primary circuitry is shown in Figure 5. The capacitor itself is charged by a nominal maximum 3000-V power supply. The capacitor is discharged into the welding circuit by a silicon controlled rectifier (SCR). As described earlier, the circuitry was designed for interfacing with a stacked core welding transformer. Use of a stacked core transformer necessitated polarity switching to prevent saturation from discharge to discharge. Therefore, a polarity switch is included just upstream from the welding transformer. The developed circuitry also contains various levels of protection circuits. This includes a passive discharge circuit for preventing stored charge on the capacitor. The passive circuit employs a 100-k Ω resistor continuously connected across the capacitor to provide continuous discharge in the event of control failure. Also included is protection to prevent current flow during under-damped conditions back into the charging power supply. Finally, the SCR gate was isolated from the rest of the power circuit. Here, a separate battery-based power supply was used for firing.

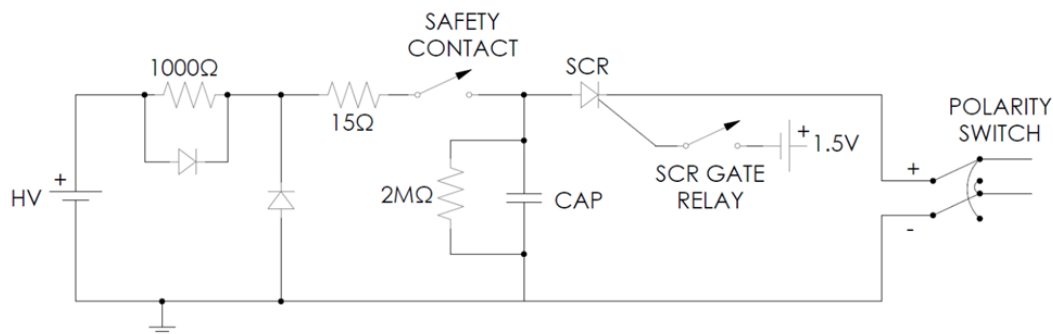


Figure 5. Schematic Diagram of the Power Supply Configuration Used for the Developed Open Architecture CD Welding System

Experimental Procedures

The developed CD power supply utilized a film-type capacitor. This unit had a capacitance value of 1280 μ F. The capacitor was energized with a TDK Lambda 102A-3KV-POS charging unit that could achieve voltages of up to 3000 V. Capacitor initiation for welding was provided by an Infineon TZ530N36KOF-EUPC 3600 V rated SCR. The SCR was fired from a nominal 1- $\frac{1}{2}$ volt, 100-ms pulse. Polarity switching was done using a Gigavac G53WF DC operated device rated up to 75 A primary current. Control of the system was accomplished with an Omega HE-XE105 programmable logic controller. This control managed capacitor charge, polarity switching, and SCR firing. All components were mounted in a NEMA 12 cabinet. This cabinet with components mounted is shown in Figure 6.

The power supply was coupled with an existing 5-kN maximum force pedestal-type resistance welding machine. This welding system is shown in Figure 7. The mechanical system on this

unit includes a nominal welding head weight of 110 kN. The unit also includes a series-stacked core transformer arrangement. The main transformer is rated at 30 kVA, and incorporates both series and parallel tap switches. On the primary side of this unit is an auto-transformer with eight additional tap switches. The resulting arrangement includes 128 possible windings configurations. With this configuration, turns-ratios could be varied from nominally 75:1 up to 1625:1. This transformer arrangement allows turns-ratio step changes to be achieved in increments of less than 10%. The transformers themselves were designed to function with AC power at voltages up to about 500 V. Prior to use in this application, the transformers underwent dielectric testing to assure stability at a maximum operating voltage of 3000 V.



Figure 6. NEMA 12 Cabinet Housing the Components of the Power Supply (the main capacitor is shown)

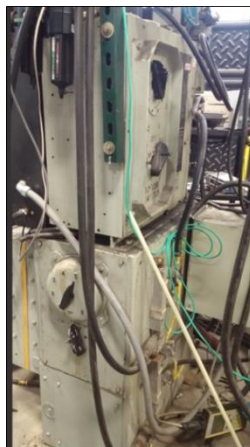


Figure 7. Welding Frame with Imbedded Transformers Used in This Study (Parallel/Series/ Auto tap switches are shown)

For evaluating the system, three projection-style weld nuts were used. The design of these weld nuts is provided in Figure 8. Included projections were nominally 2.5 mm in diameter and 1 mm tall. Nuts themselves were of mild steel, and welded to 0.8-mm sheet stock of similar material. During these studies, welded nuts were evaluated by push-off testing. This was done in a Southwark hydraulic tensile testing machine. Testing was done at nominally 7.5 mm/min.

Load to failure was used as the measure of joint quality. A sample failed joint is shown in Figure 9. Representative samples were also sectioned and examined metallographically. Metallographic sample preparation was performed using standard techniques. Samples were etched in Nital to reveal the underlying microstructures.

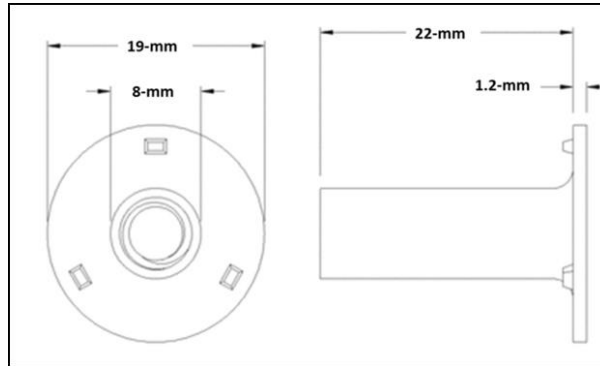


Figure 8. Engineering Details of the Weld Nut Used in This Study (actual projections are nominally 2.5 mm in diameter and 1 mm tall)



Figure 9. Actual Nut Welded to a 0.8-mm Sheet Steel Following Push-Off Testing

Results

Actual welding trials were conducted to evaluate the differences of process waveforms on the application of interest. From the available range of windings ratios on the transformer, two were selected for evaluation. These included 103:1 and 213:1. This nominal 2:1 difference in windings ratio suggests a similar difference in current rise times as suggested in the analysis section above. Trials were conducted as a set of “current range” tests. These included setting baseline parameters (welding force, turns-ratios) then increasing charge voltages/discharge currents while measuring changes in weld performance. Data from the current range studies is provided in Table 2. All trials were done with a constant weld force of 3.3 kN. Testing was done by first selecting the turns-ratio, and then increasing voltages from the no-weld condition to expulsion. Included in the table are the charge voltages, resulting currents, estimated time to peak currents, and measured push-off strengths.

Table 3. Current Range Data for the Two Turns-Ratio Configurations Selected for Study (table includes process responses of measured peak currents, rise times, and push-off strengths).

Weld Force (kN)	Charge Voltage (V)	Turns-Ratio	Current (kA)	t_p (ms)	Push off test (kN)	Comments
3.3	250	103	5.4	3.3	0.0	No weld
3.3	400	103	9.3	3.0	0.1	No buttons
3.3	500	103	11.7	3.2	2.3	No buttons
3.3	600	103	14.9	3.2	2.7	3 buttons pulled
3.3	600	103	15.0	2.8	3.4	3 buttons pulled
3.3	600	103	15.5	2.7	n/a	Met sectioned
3.3	700	103	18.1	3.4	2.7	3 buttons pulled
3.3	800	103	20.4	3.5	2.9	3 buttons pulled
3.3	500	213	7.3	4.7	0.0	No weld
3.3	600	213	9.6	4.4	0.0	No weld
3.3	700	213	10.6	5.1	2.5	No buttons
3.3	800	213	11.9	5.0	3.4	3 buttons pulled
3.3	900	213	14.4	6.0	4.1	3 buttons pulled
3.3	1000	213	16.9	6.4	3.8	3 buttons pulled
3.3	1000	213	17.1	6.0	n/a	Met sectioned
3.3	1100	213	19.6	5.7	4.0	3 buttons pulled
3.3	1200	213	21.4	6.7	3.8	3 buttons pulled

A key aspect to note on this table is the differences in characteristic current rise times. For the 103:1 turns-ratio, rise times averages about 3 ms. For the higher turns-ratio (213:1), those rise times were nearly double, averaging 6 ms. This is consistent with the modeling discussion above.

Process range results, (with push-off strengths as the dependent variable) are provided in Figures 10 and 11. Figure 10 shows the variations in push-off strengths as the charge voltage is increased for the two different turns-ratios. These results show that initially, welding takes place at lower charge voltages for the lower transformer turns-ratio. This is not surprising, as the lower turns ratio results in higher secondary voltages (and currents) for a given charge value. Of additional interest are the achieved maximum strengths for the two turns-ratio trial sets. Those welds made at the higher turns ratio (213:1) show peak strengths of roughly 4 kN compared to 3 kN for similar trials at 103:1. The same strength data plotted in terms of welding current are provided in Figure 11. The data here suggest that the current ranges for the two turns-ratios studied are similar. The differences in peak loads for the two turns-ratios described earlier are evident.

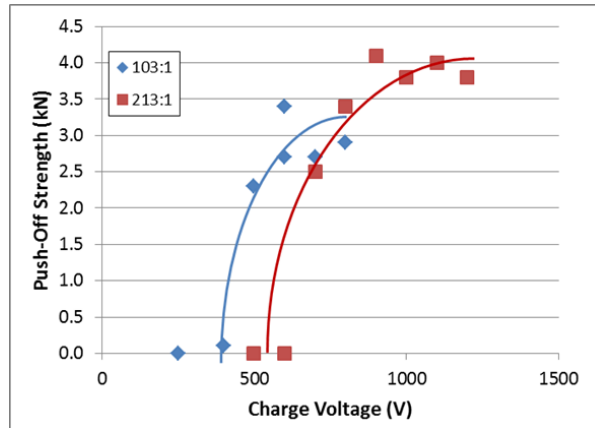


Figure 10. Process Range Based on Charge Voltage for Two Different Transformer Turns-ratios (ratios include 103:1 and 213:1)

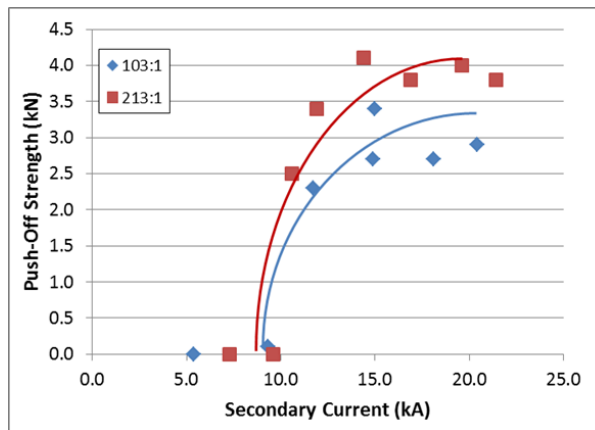


Figure 11. Process Range Based on Secondary Current for Two Different Transformer Turns-ratios (ratios include 103:1 and 213:1)

Characteristic secondary current waveforms taken from each of these sets of trials are provided in Figures 12 and 13. In each case, waveforms are provided from conditions representing the top and bottom of the current range. Figure 12 provides the waveforms from the 103:1 turns-ratio trials. Specific samples include those taken at 400-V and 800-V charge voltages. The resulting waveforms appear to be overdamped, with peak currents in proportion to the charge voltages used. The higher voltage waveform also demonstrates a slightly longer rise time, and faster decline in current after the peak value is achieved. Similar results from the 213:1 trials are provided in Figure 13. Here, the limit of the current range curve was defined by charge voltages of 600 and 1100 V. Again, the peak currents roughly scaled with the charge voltage. Again, higher charge voltages resulted in slightly longer rise times (and faster current decay rates). Of interest are the differences between the curves for the two different turns-ratios. While the upper and lower current limits were similar, the higher turns-ratio results showed longer rise times, significantly extended total current durations, and a transition from an overdamped to an under-damped response condition.

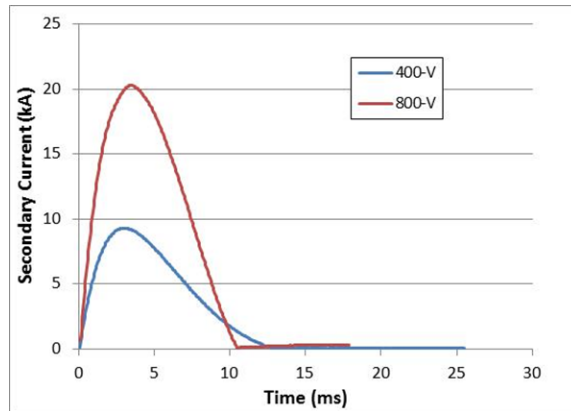


Figure 12. Secondary Current Waveforms for Welds Made at High and Low Voltage Values Using a 103:1 Turns-ratio

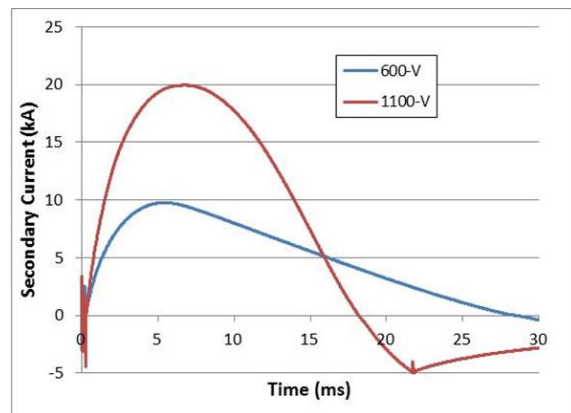


Figure 13. Secondary Current Waveforms for Welds Made at High and Low Voltage Values Using a 213:1 Turns-ratio

Macro- and micro-structures from welds made at the top of the current range with the two turns-ratio arrangements are provided in Figures 14 – 17. Figures 14 and 15 present macro- and micro-sections of the welds made at the 103:1 turns-ratio, respectively. The macrograph of this weld shows relatively shallow projection collapse (~one fifth the projection height). Further, the heat-affected zone on the nut appears to penetrate only about one half the retained projection height. Alternately, the apparent heat-affected zone on the sheet side of the joint is limited to about one half the thickness. Details of the bondline microstructure (Figure 15) indicate a fully solid-state joint. This is evidenced by: 1) the lack of any discernable fusion zone, 2) the lack of any apparent solidification structure, and 3) the apparent remnant bondline in the micro-structure. On the nut side of the joint, the micro-structure is dual phase, including both retained ferrite and austenite grains that have transformed to either acicular ferrite or martensite on cooling. The sheet side of the joint is characterized primarily by ferrite grain growth.

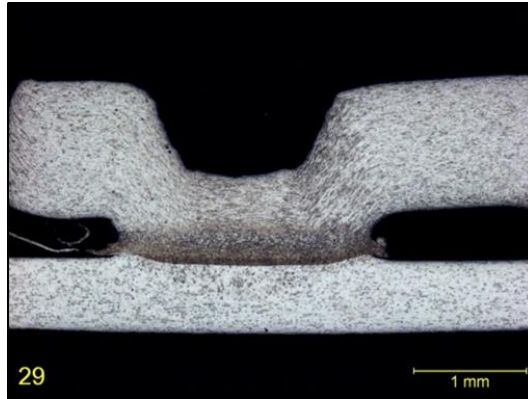


Figure 14. Macrostructure of a CD Weld Made Using a Turns-ratio of 103:1 (note shallow set-down and extents of heat-affected zone formation)



Figure 15. Microstructural Details of the Bondline on a CD Weld Made with a Turns-ratio of 103:1 (note retained ferrite on both sides of the joint)

Figure 16 presents the macro-structure of the joint made with a 213:1 turns-ratio. Compared to the lower turns-ratio joint, the current levels are slightly higher (17.1 vs 15.5 kA), set-down of the projection is greater, and heat-affected zones into both the nut and attached sheet are more pronounced. On the nut-side of the joint, the heat-affected zone can be seen to extend completely to the projection base, with bands indicating differing fractions of austenite formation (and decomposition on cooling). On opposite side the heat affected zone appears to achieve full penetration of the attached sheet. A high magnification micrograph of the bond line is provided in Figure 17. In this case, the nut-side of the joint completely consists of prior austenite grains. The sheet-side of the joint is still dominated by ferrite grain growth, but there are indications of acicular ferrite (suggesting austenite formation and decomposition) within a few microns of the bond line. It is also of note that there are small islands of recrystallized material (presumably prior austenite) along the bond line. Some of these appear to have pitted during etching.

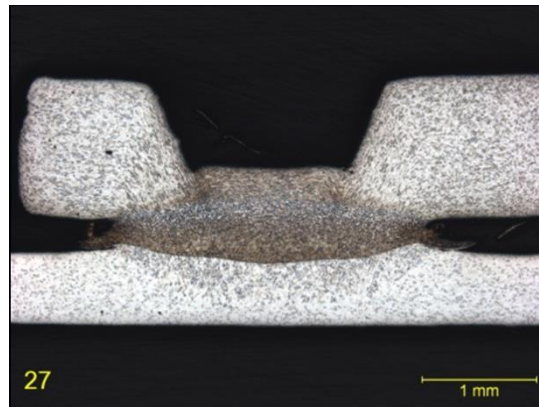


Figure 16. Micro-structural Details of the Bondline on a CD Weld Made with a Turns Ratio of 213:1 (note acicular ferrite on both sides of the joint indicating prior austenite)

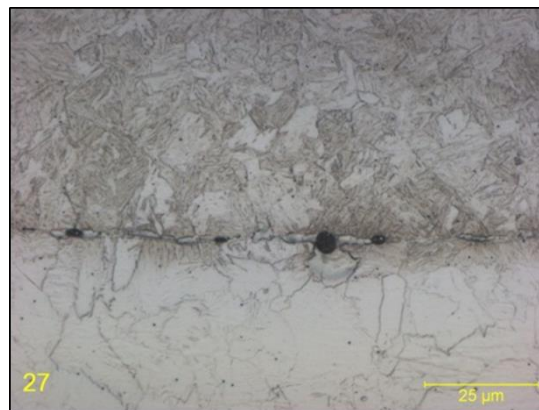


Figure 17. Micro-structural Details of the Bondline on a CD Weld Made with a Turns Ratio of 213:1 (note acicular ferrite on both sides of the joint indicating prior austenite)

Discussion

As stated previously, CD welding is a combination of electrical and mechanical responses to achieve localized heating and subsequent forging to create a joint. In this study, an engineering tool has been developed to allow precise and controlled variations in each element of both the electrical and mechanical sub-systems of the CD welding process. This allows optimization of the main factors affecting CD welding of any specific application. These include:

1. The peak current
2. The current rise time
3. The weld head weight to welding force ratio

How these factors interact has been demonstrated by applying the capabilities of this open architecture system to a sample weld nut application. For this application, the results suggest joint strength is benefited by slower rise times (here 6 ms compared to 3 ms), though best practice peak welding currents remained a constant (~20 kA). This longer rise time has resulted

in both greater collapse of the projection itself, as well as heat penetration into the substrates. Welds with these slower rise times appeared to result in peak strength values roughly 30% greater than those using the faster ones.

Analysis of these results suggests that the third factor described above is playing a role in the observed response that is the influence of the weld head weight itself. The influence of head weight and its relationship to projection collapse is described elsewhere⁽²⁾. That work provides a method to estimate allowable collapse distances (motion of the parts together without losing more than 5% of the applied weld force) as a function of the applied force, head weight, and observed rise times from the experimental trials. That criterion, adapted to the welding forces and welding system head mass employed in this study is shown in Figure 18.

This analysis indicates that for the trials conducted with nominally 3-ms rise times (103:1 turns ratio) a maximum stable collapse distance of ~0.14 mm could be achieved. For the 6-ms rise time trials (213:1), the stable collapse distance increases to slightly over 0.5 mm. These numbers are strikingly similar to the observed collapse distances seen in the macrographs taken for these two sets of trials. It is of note that at greater apparent collapse distances effective contact forces decrease, leading to expulsion. This leads to inconsistent behavior on mechanical testing. Alternately, allowing larger stable collapse distances (either through slower rise times or lower head weight to weld force ratios) offers potential for larger bond areas and higher strengths. Both observations are consistent with mechanical properties data collected in this study.

It is further of note that the CD process itself is largely defined by peak currents and associated rise times. These values (rise times and peak currents) suggest differing energy inputs into the weld. This is clear from overlaying process waveforms using different rise times, but achieving similar currents. This is done in Figure 19 for conditions at each of the two turns ratios yielding peak currents of roughly 20 kA. The differences in discharge energy content under the two curves are clear. In the lower turns-ratio case, the energy used is about 400 J. For the higher turns ratio case, the energy used almost doubles (770 J). This difference in energy is of course still dissipated as heat in the weld, and corresponds to the divergent heat-affected zone extents for the two sets of trials.

Clearly, proper optimization of capacitive discharge welding is a function of a range of factors, including part (projection) design, materials, required tooling, system reach, etc. These factors then define characteristics of the welder secondary, including load resistance (R_s) and inductance (L_s). The analysis and results presented above suggest that proper selection of system capacitance, charge voltage, and windings ratio can be used to achieve desired currents and rise times over a wider range of these secondary characteristics. This then, allows opportunity for enhanced CD weld process optimization for individual applications.

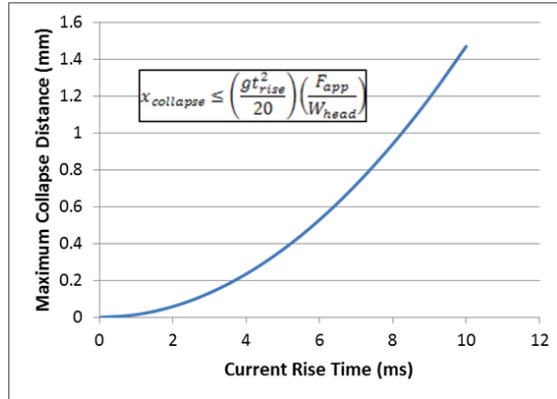


Figure 18. Relationship between the Maximum Allowable Collapse Distance and Rise Time for the Welding System Used in This Study

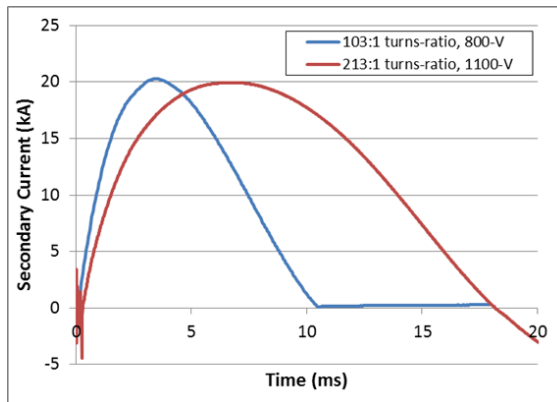


Figure 19. Comparison of Current Pulses Achieving 20 kA for Two Different Transformer Turns Ratios

The open architecture CD welding system developed in this study offers considerable flexibility on how the process is configured. The system allows independent variation in the levels of capacitances used, charge voltages, transformer turns-ratios, welder secondary geometries, weld head configurations, and applied forces. This then provides the opportunity to experimentally examine and optimize candidate applications. Resulting practice optimizations can then be transferred to specific system designs allowing better application of this class of technology in manufacturing.

Conclusions

In this work, an open architecture capacitive discharge welding system has been conceptualized, designed, assembled, and demonstrated. The system design is based on supplying a polarity switched CD-based current pulse to a stacked-core transformer arrangement. This resulted in a system with wide flexibility in matching power supply outputs to secondary loading. The system was demonstrated on a candidate weld nut application. Trials were conducted to show the influence the different secondary current profiles achievable with system. Specific conclusions from this program include:

1. Specific combinations of capacitance, charge voltages, and turns ratios could be used to match peak currents and rise times across applications – This was demonstrated through electrical analysis and validated with experimental studies.
2. A system was designed and developed integrating a capacitive discharge power supply with an existing stacked-core transformer arrangement – The system allowed rapid change-out of capacitors and use of a transformer with parallel/series tap settings. This system included an upstream 8-tap autotransformer for total of 128 separate turns ratios.
3. Increasing transformer windings ratios affect reflected inductances from secondary to primary, resulting in longer rise times – Windings ratios of 103:1 and 213:1 were employed in this study, with resulting rise times of 3 and 6 ms, respectively.
4. Welding with either rise time showed similar current ranges – For both rise times, initial strengths and expulsion were seen at roughly 9 and 20 kA, respectively.
5. Charge voltages were significantly higher for the trials done at the higher windings ratio – Doubling the windings ratio effectively doubled the necessary charging voltage to hit similar currents.
6. Peak strengths for the longer rise time trials were significantly higher than those done with short rise times – Peak strengths for the trials done with the 213:1 turns-ratio (6-ms rise time) were roughly 30% higher than those done with the 103:1 turns-ratio (3-ms rise time).
7. Degrees of set-down were correlated with the rise times used – Maximum set-downs for the trials performed with the 103:1 (3-ms rise time) and 213:1 (6-ms rise time) turns-ratios were about one fifth and one half the projection height, respectively.
8. Achievable set-downs without expulsion were limited by secondary mechanical considerations – The weld head weight/weld force ratio in these studies was constant at roughly 3.3%. Analysis showed that this was consistent with roughly 0.14 and 0.52-mm set-down in for the 3 and 6-ms rise times, respectively. This was consistent with the metallographic results.
9. Increased set-downs led to larger bond areas and higher joint strengths – Use of shorter rise times must be balanced with proper design of the welding heads for best performance.
10. The variables employed in the open architecture CD system allow tuning of process waveforms for specific applications – Flexibility in turns-ratios and charge voltages allowed controlled process waveforms facilitating independent control of peak currents and rise times specific applications.

References

1. Resistance Welding Manual, Fourth Edition. *Resistance Welding Manufacturing Alliance*, Philadelphia, Pennsylvania, 1989.
2. Gould, J.E., “Mechanisms of solid-state resistance welding”, *ASM Handbook*, Vol. 6, Part A: Welding Fundamentals and Processes, pp. 171-178, Metals Park, Ohio, 2011.

3. Alberti, H. and Früangel, F., „Das widerstandschweißen mittels transformierter kondensatorentladung“, *Blech*, Vol. 8, No. 9, pp. 678-685, 1961.
4. Galcinskij, L.V., „Besonderheiten des kondensatorpunktschweissens und möglichkeiten seine anwendung“, *Schweisstechnik*, Vol. 34, No. 12, pp. 552-553, 1984.
5. ~~Merkblatt DVS 2911~~ Kondensatorentladungsschweißen – Grundlagen, Verfahren und Technik, *Merkblatt DVS 2911*, DVS, Düsseldorf, Deutschland, 2016.
6. Klemperer, H., „Capacitor -discharge welding systems“, *Electronics*, Vol. 17, No. 5, pp. 118-121, 1944.
7. Salser, T.E., Briefer, D.K., and Becker, G., „High current, low impedance resistance welding device“, United States Patent 6756558 B2, 2004.